VIRULENCE
2025, VOL. 16, NO. 1, 2474185
https://doi.org/10.1080/21505594.2025.2474185

Taylor & Francis
Taylor & Francis Group

BACTERIAL PATHOGENESIS

OPEN ACCESS Check for updates

The molybdate transport protein ModA regulates nitrate reductase activity to increase the intestinal colonization and extraintestinal dissemination of *Klebsiella pneumoniae* in the inflamed gut

Jichen Xie[a*], Hui Wang[a*], Renhui Ma[a], Jinming Fan[a], Qiuhang Quan[a], Zhiqiang Zhang[a], Moran Li [a,b], and Bei Li[a,c,d]

[a]School of Basic Medical Science, Hubei University of Medicine, Shiyan, China; [b]Department of Respiratory, Renmin Hospital, Hubei University of Medicine, Shiyan, China; [c]Biomedical Research Institute, Hubei University of Medicine, Shiyan, China; [d]Department of obstetricsl, Maternal and Child Health Hospital, Hubei University of Medicine, Shiyan, China

ABSTRACT

The mammalian intestine is a major site of colonization and a starting point of severe infections by *Klebsiella pneumoniae*. Inflammatory bowel disease (IBD) is an inflammatory disorder of the gut, and host-derived nitrate in IBD confers a luminal growth advantage upon *Escherichia coli* and *Salmonella typhimurium* through nitrate respiration in the inflamed gut. However, the impact of nitrate on the growth and pathogenicity of *K. pneumoniae* in this microenvironment is poorly understood. In this study, we used oral administration of dextran sodium sulphate to induce IBD in mouse models. We then analysed the colonization levels of *K. pneumoniae* wild-type (WT), the nitrate reductase gene mutant strains (Δ*narG*, Δ*narZ* and Δ*narG*Δ*narZ*), and the molybdate uptake gene mutant strain (Δ*modA*) in the inflamed intestinal tract. Results showed that the growth, intestinal colonization, and extraintestinal dissemination of *K. pneumoniae* were increased in the intestines of dextran sulphate sodium (DSS)-treated mice. Nitrate in the inflamed bowel conferred a growth advantage to *K. pneumoniae* through nitrate respiration. The molybdate transport protein ModA regulated nitrate reductase activity to increase the growth, intestinal colonization, and extraintestinal dissemination of *K. pneumoniae*. Tungstate will be a promising antibacterial agent to tackle *K. pneumoniae* infections in IBD patients.

ARTICLE HISTORY
Received 6 February 2024
Revised 24 January 2025
Accepted 25 February 2025

KEYWORDS
IBD; *Klebsiella pneumoniae*; ModA; nitrate reductase; intestinal colonization

Introduction

Klebsiella pneumoniae is a facultative anaerobe that can colonize the mucosal epithelium of the human intestinal tract and oropharynx. The intestinal tract serves as the starting point of severe infections, such as pyogenic liver abscesses, meningitis, and endophthalmitis, caused by *K. pneumoniae* [1–4]. To survive and establish colonization in the host's gastrointestinal tract, bacteria must overcome biological stresses and adapt metabolically to the host intestinal environment. The intestine is a hypoxic environment, and alternative electron acceptors (AEAs) such as dimethyl sulphoxide (DMSO), trimethylamine N-oxide (TMAO), and nitrate (NO_3^-) are required to fuel oxidative phosphorylation for the growth of facultative anaerobes [5]. These AEAs are by-products of gut inflammatory responses and confer a growth advantage to some facultative anaerobes through anaerobic respiration.

Inflammatory bowel disease (IBD) is a chronic recurrent intestinal inflammatory disease, and the nitrate level is elevated during gut inflammation. Host-derived nitrate can be utilized by *Escherichia coli* and *Salmonella typhimurium* for anaerobic nitrate respiration to confer a fitness advantage in the inflamed gut [6–8]. Nitrate reductases are the key enzymes involved in nitrate respiration, and their activities require the incorporation of an essential molybdenum cofactor (MoCo) into the active site [9–11]. In most bacteria, the high-affinity uptake of molybdate from the environment to form MoCo depends on the molybdate uptake system, ModABC [12–14]. In *E. coli* and *Pseudomonas aeruginosa*, loss of Mo uptake results in reduced nitrate reductase activity and impaired growth on nitrate-containing media [6,15]. Compared to a ModABC system and three nitrate reductases in *E. coli*, the *K. pneumoniae* genome contains a ModABC molybdate uptake system and two nitrate

CONTACT Moran Li moranli@whu.edu.cn; Bei Li libei2381@sina.com School of Basic Medical Science, Hubei University of Medicine, 30 South Renmin Road, Shiyan, China
*Jichen Xie and Hui Wang contributed equally to this work.

reductases encoded by the *narGHI* and *narZYV* genes [16]. Little is known about the roles of nitrate in *K. pneumoniae* growth and pathogenicity in the intestinal microenvironment.

In patients with IBD, the prevalence of *K. pneumoniae* gastrointestinal carriage and the incidence of pyogenic liver abscess infections have increased compared to those in the control cohort [17–19]. Given the rising multidrug resistance, new strategies are needed to control the colonization and prevent infection of *K. pneumoniae*. The mechanisms by which IBD increases *K. pneumoniae* colonization in the gastrointestinal tract need to be better understood. This study used oral administration of dextran sodium sulphate (DSS) to induce IBD in mouse models. Moreover, we analysed the colonization levels of *K. pneumoniae* wild-type (WT), the nitrate reductase gene mutant strains (Δ*narG*, Δ*narZ* and Δ*narG*Δ*narZ*), and the molybdate uptake gene mutant strain (Δ*modA*) in the inflamed intestinal tract. This study aims to explore the roles of nitrate respiration and the molybdate uptake protein ModA in the growth and pathogenicity of *K. pneumoniae* in IBD patients. Due to the structural similarity between tungstate and molybdate, tungsten can inactivate nitrate reductase by competitively binding to ModA and replacing Mo in the MoCo [15,20]. It has been shown that tungstate can eliminate the fitness advantages of MoCo-dependent anaerobic respiration and selectively inhibit the expansion of Enterobacteriaceae to ameliorate colitis [21]. Therefore, the effect of tungstate as an antibacterial agent in decreasing *K. pneumoniae* infections in IBD patients will be studied.

Methods

Bacteria and culture conditions

Bacteria, plasmids, and primers used in the present study are summarized in Table 1. All *K. pnemoniae* strains were cultured overnight in Luria-Bertani (LB) broth at 37°C and 200 rpm, then diluted 1:100 into fresh LB broth and cultured to an optical density at 600 nm (OD_{600}) of 1.2 for standardization. For growth assays *in vitro*, the standardized cultures were diluted 1:100 into AT minimal medium containing 2 g $(NH_4)_2SO_4$, 0.078 g $MgSO_4$, 7.6 mg $CaCl_2$, 5 mg $FeSO_4$-7 h_2O, 2.2 mg $MnSO_4$-H_2O, 10.7 g KH_2PO_4 (pH 7.3), 1 mL 20 mm $FeCl_3$ and 2 mL freshly prepared glycerol per litre [22]. For anaerobic growth, 20 mm KNO_3

Table 1. Bacterial strains, Plasmids, and primers used in this study.

Bacteria and plasmids	Description	Reference or Source
Bacteria		
K. pneumoniae		
NTUH-K2044 (WT)	Wild-type strain; Ap^r; parent strain for generation of isogenic mutant strains	[23]
Δ*modA*	Deletion of *modA* from WT; Ap^r	Present study
C-*modA*	Complemented *modA* mutant; Ap^r; Km^r	Present study
Δ*narG*	Deletion of *narG* from WT; Ap^r	Present study
Δ*narZ*	Deletion of *narZ* from WT; Ap^r	Present study
Δ*narG*Δ*narZ*	Deletion of *narG,narZ* from WT; Ap^r	Present study
Plasmids		
pKO_3-Km	pKO_3-derived plasmid, with an insertion of Km resistance cassette from pUC4K into *AccI* site	[25]
pGEM-T-easy-km	pGEM-T easy with an insert of Km cassette from pUC4K into *NdeI* site	[26]
Primers		
modA Mutant constructs		
modA-A	GTATGCGGCCGCATCCACCAACGGATGTTCGC	
modA-B	GCCCTTTCAGGTAGTCATAGCTTACTCTCCTGTCAATGCG	
modA-C	CGCATTGACAGGAGAGTAAGCTATGACTACCTGAAAGCGC	
modA-D	GTATGCGGCCGCCAACGGCAACGTAATGGTC	
modA-F	ATGGCAGGTTCTTGGTTACG	
modA-R	ACTTTCTGATGCGAGGCTTC	
Complemented *modA* mutant		
C-*modA*-F	ATGGGCCCGAGATGGCCGCCAGCAGG	
C-*modA*-R	TAAAGCGGCCGCTCAGCGGGTGGTAAATCCGT	
narG Mutant constructs		
narG-A	GTATGCGGCCGCTTCGGTATCTCGCTGGAT	
narG-B	TTACGCTCTCCTGTACCTGGCGGGTTTCTCCTGATATGG	
narG-C	CCATATCAGGAGAAACCCGCCAGGTACAGGAGAGCGTAA	
narG-D	GTATGCGGCCGCAGGATCTCTTCCCAGTTCG	
narG-F	ATGAAGATGTGGCGGGAAG	
narG-R	GCAGAGTTTGGCGATTTCG	
narZ Mutant constructs		
narZ-A	GTATGCGGCCGCCTCCACCTTCCAGATGATCG	
narZ-B	GTACCTGATCGCGACCTTGACATTTCTCCTGCTCCGAT	
narZ-C	ATCGGAGCAGGAGAAATGTCAAGGTCGCGATCAGGTAC	
narZ-D	GTATGCGGCCGCCCATCTTCCTCACGCTTGTAGA	
narZ-F	CCAGCAGTTGTATCAGGACC	
narZ-R	ACCGAGTTATGAATGCCG	

(Aladdin) was added to AT medium, and 100 μM Na_2MoO_4 or 10 mm Na_2WO_4 (Aladdin) was added as needed, followed by incubation in a compact anaerobic workstation DG250 (Don Whitley Scientific Ltd, Shipley, Hampshire, UK) for continuous culture. For intestinal infection, the standardized cultures were diluted 1:100 into fresh LB broth and cultured to an OD_{600} of 2.0 with a 10-fold enrichment. *E. coli* DH5α was used as a cloning host and grown in LB medium.

Construction of deletion mutants and complemented strain

The deletion of *modA*, *narG*, and *narZ* from *K. pneumoniae* NTUH-K2044 (WT) [23] were carried out using the homologous recombination method described previously [24]. The left and right flanking sequences of *modA*, *narG*, and *narZ* were cloned into the temperature-sensitive suicide plasmid pKO_3-km [25] (with the sucrose-lethal gene *SacB*), and then electrotransformed into the WT strain. The successful integration of the flanking sequences into the chromosome was selected by growing the transformants on LB agar at 43°C. Several positive transformants were subcultured at 30°C with sucrose to eliminate the plasmid. The double knockout strain Δ*narG*Δ*narZ* was generated by deleting *narZ* from the Δ*narG* mutant. A 1,594-bp DNA sequence containing the promoter, coding region, and terminator of *modA* was cloned into pGEM-T-easy-km [26] and electrotransformed into Δ*modA* to construct the complemented strain C-*modA*.

Nitrate reductase activity assay

The nitrate reductase activity of the *K. pnemoniae* strain was assayed as described by Hughes et al. with minor modifications [27]. Briefly, bacterial cultures were grown anaerobically in an AT medium supplemented with or without 20 mm KNO_3 for 3 h. Sixty μL of the cultures were transferred into 96-well plates, and a BioTek microplate reader (BioTek, Winooski, Vermont, USA) was used to measure OD_{600}. Then, 60 μL of 1% (w/v) sulfanilic hydrochloride (prepared in 18% HCl) and 0.1% *N*-(1-Naphthyl) ethylenediamine dihydrochloride were added, respectively. The samples were incubated for 10 min in the dark after mixing. OD_{540} and OD_{420} were measured, and the nitrate reductase activity was calculated using the following formula:

Nitrate reductase activity = $(OD_{540} - 0.72 \times OD_{420})/(0.18 \times 3 \times OD_{600})$.

DSS-induced colitis model, K. pneumoniae intestinal infection, and tungstate treatment

Female 7- to 9-week-old C57BL/6 mice were purchased from HUNAN SJA Laboratory Animal Co., Ltd. Groups of C57BL/6 mice received either sterilized water (Mock) or a 3% (w/v) dextran sulphate sodium (DSS; molecular weight 36,000–50,000; MP Biomedicals) solution (dissolved in sterilized water and then filtered) for 8 d. For tungstate treatment, mice were administered 3% DSS and 0.2% (w/v) Na_2WO_4 solution. The experiment involved daily observation of mouse faeces and recording body weight. Drinking water was switched to sterilized water 24 h before the end of the experiment for DSS-treated mice. Mice were inoculated intragastrically with 0.1 mL of LB broth containing 1×10^9 CFU of *K. pneumoniae* strains on day 5. Faecal samples were collected at 24 and 48 h post-inoculation from 4 to 5 mice per group, weighed, and evenly suspended in 1 mL of sterilized phosphate-buffered saline (PBS). Serial 10-fold dilutions were plated on LB agar plates to determine the bacterial loads. At 72 h post-inoculation, mice were euthanized and dissected. The liver, small intestine, and large intestine were collected, weighed, and homogenized in 2 mL of PBS using a tissue homogenizer. Serial 10-fold dilutions were plated on LB agar plates to calculate the bacterial loads.

Determination of nitrate concentrations in the cecal mucus layer

The nitrate concentrations in the caecal mucus layer were determined as described by Winter et al. with minor modifications [6]. Two groups of C57BL/6 mice received either water ($n = 10$) or 3% DSS ($n = 12$). Once successful induction of the colitis model was confirmed, the mice were euthanized on day 5. The caecum segments were dissected from the abdomen and weighed after carefully squeezing out the luminal contents. The caecum was then longitudinally cut, washed with PBS three times, and the mucus layer was gently scraped with a surgical blade. The caecal mucus was collected with 0.2 mL deionized water and centrifuged at 20,000 × g for 2 min at 4°C to remove larger particles. If not analysed immediately, the supernatant was sterilized by filtration and stored at −80°C. The obtained samples were mixed with a modified Griess reagent (0.1 g sulphanilamide, 0.25 g vanadium (III) chloride, 0.005 g *N*-(1-Naphthyl) ethylenediamine dihydrochloride in 100 mL of 0.5 M HCl) in a 1:1 ratio and derivatized at room temperature for 8 h. The absorbance of the reaction solution was measured at 540 nm. Meanwhile, serial 2-fold dilutions of sodium nitrate were prepared and treated as

above to generate a standard curve. The nitrate concentration in the caecal mucus layer was calculated based on the standard curve.

Competitive index assay

The plasmid pLac-EGFP, containing an enhanced green fluorescent protein gene, and pBBR1MCS2-Tac-mCherry, containing a red fluorescence protein gene, were transformed into *K. pnemoniae* WT and the deletion mutants (Δ*modA*, Δ*narG*, Δ*narZ* or Δ*narG*Δ*narZ*). An equal mixture of WT and the respective deletion mutant was then inoculated into AT broth supplemented with or without 20 mm KNO_3, and incubated anaerobically at 37°C for 24 h. The cultures were serially diluted 10-fold and spread on LB agar plates. The colonies were identified and counted using a fluorescence microscope (General Electric Company, Boston, Massachusetts, USA). The competitive index was calculated by dividing the CFU of the recovered WT by the CFU of the deletion mutant. In a separate experiment, an equal mixture of WT and Δ*modA* mutant was inoculated into AT broth containing 20 mm KNO_3 supplemented with or without 10 mm Na_2WO_4 for tungstate treatment.

Ethics statement

All animal experiments were approved by the Animal Care and Use Committee of Hubei University of Medicine (Reference Number: HBMU 2019–061) and complied strictly with the ARRIVE guidelines (https://arriveguidelines.org/).

Statistical analyses

The bacterial counts were log-transformed before analysis. The statistical differences between two groups were determined using an unpaired two-tailed Student's *t*-test, while differences between multiple groups were assessed using one-way analysis of variance (ANOVA). For the competitive index assay, a paired two-tailed Student's *t*-test was used.

Results

The ability of intestinal colonization and extraintestinal dissemination of K. pneumoniae are increased in the inflamed gut

Oral administration of DSS was used to induce the IBD mouse model. The DSS-treated mice exhibited bloody, loose faeces and significant weight loss on day 4 (Figure 1(a)), suggesting the successful induction of the IBD model. After intragastric inoculation with 1×10^9 CFU of the *K. pneumoniae* WT strain, bacterial numbers in the faecal contents of DSS-treated mice were higher than those in placebo-treated mice (24 h: 10-fold, $p = 0.035$; 48 h: 1000-fold, $p = 0.0027$) (Figure 1(b)). Furthermore, the bacterial loads in the liver, large intestine, and small intestine of DSS-treated mice at 72 h post-inoculation were approximately 14, 60, and 100 times as those of the control group, respectively (Figure 1(c)). These results suggest that *K. pneumoniae* is more likely to proliferate and breach the intestinal barrier in DSS-treated mice, thus infecting the extra-intestinal tissues such as the liver. Overall, these findings indicate that *K. pneumoniae* exhibits enhanced intestinal colonization and extraintestinal dissemination in the inflamed gut.

Nitrate concentrations in the intestinal lumen are elevated in the inflamed gut

Nitrate, a by-product of the host inflammatory response, serves as a terminal electron acceptor to boost the growth of *E. coli* in the inflamed gut [6]. To assess the impact of intestinal nitrate on the development and pathogenicity of *K. pneumoniae*, the nitrate concentrations in the caecal mucus layer of mock-treated and DSS-treated mice were measured. The nitrate levels in DSS-treated mice were significantly higher than those in mock-treated mice (~2-fold, $p = 0.0001$, Figure 2), suggesting that the increased susceptibility of mice with IBD to intestinal infection by *K. pneumoniae* may be related to elevated nitrate production during gut inflammation.

The in vitro anaerobic nitrate environment promotes the growth of K. pneumoniae

To investigate the effect of intestinal nitrate on the growth of *K. pneumoniae*, 20 mm KNO_3 was added to AT medium containing glycerol as the carbon source to simulate the nitrate-rich environment of gut inflammation *in vitro*. The aerobic growth of the WT strain was not affected by the addition of nitrate (Figure 3(a)), while its anaerobic growth was significantly enhanced throughout the growth stage (Figure 3(b)). Furthermore, nitrate reductase activity was undetectable after 3 h of anaerobic culture of the WT strain in AT medium without KNO_3. In contrast, the addition of nitrate significantly increased nitrate reductase activity (Figure 3(c)). These results suggest that nitrate promotes anaerobic growth of *K. pneumoniae* by inducing nitrate reductase expression, providing a growth advantage in the inflamed gut through nitrate respiration.

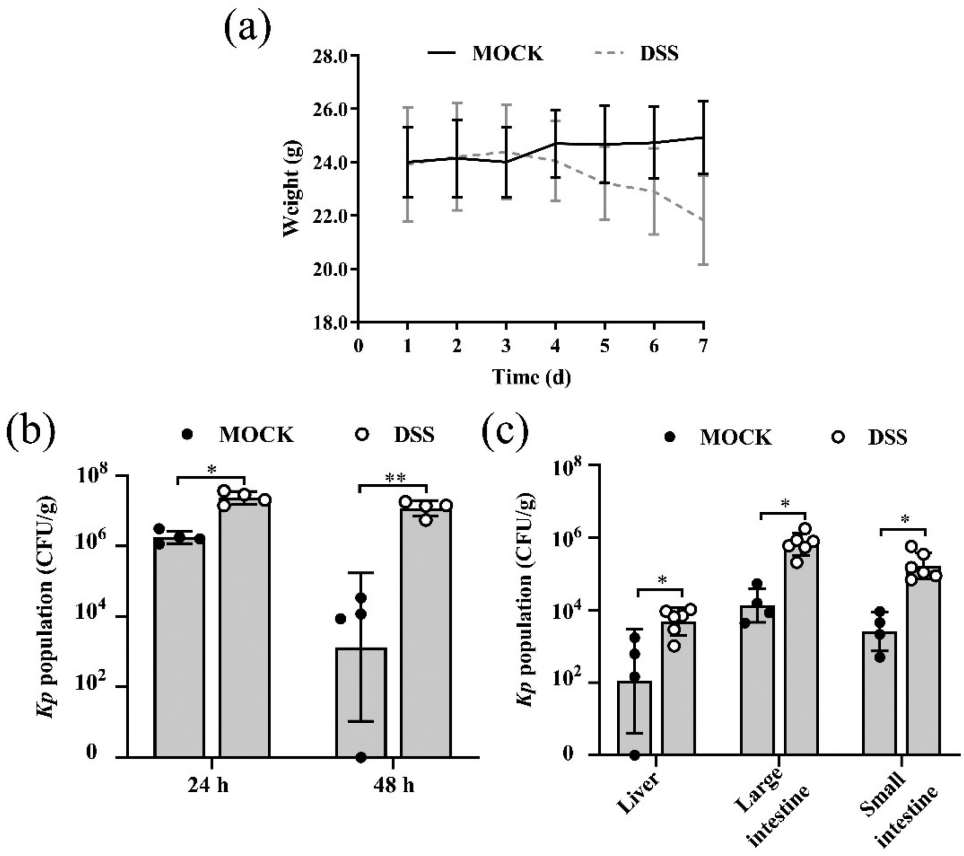

Figure 1. The intestinal colonization and extraintestinal dissemination of *K. pneumoniae* are increased in the dss-induced IBD mouse model. Groups of SPF C57BL/6 mice were administered 3% DSS (DSS group) or water (mock group), and then inoculated intragastrically with 10^9 CFU of *K. pneumoniae* NTUH-K2044 wild-type strain (WT) on day 5. (a) Body weight changes of the mice were monitored throughout the experiment. (b) Fecal bacterial counts of mice were determined at 24 and 48 h post-inoculation with the WT strain. (c) Bacterial loads in the liver, large intestine, and small intestine tissues were calculated 72 h after inoculation. Data are represented as means ± standard deviations (error bars). *,$p < 0.05$; **,$p < 0.01$ (unpaired two-tailed Student's *t*-test).

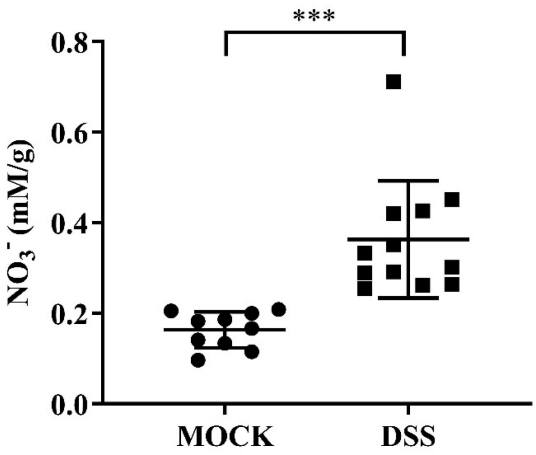

Figure 2. Nitrate concentration (NO_3^-) in the caecal mucus layer of mock and dss-treated mice. C57BL/6 mice were divided into two groups: one receiving water (mock, $n = 10$) and the other 3% DSS (DSS, $n = 12$). On day 5, mice were euthanized, and caecum segments were dissected from the abdomen. The caecal mucus layer was collected, and nitrate concentrations were measured. ***,$p < 0.001$ (unpaired two-tailed Student's *t*-test).

Nitrate respiration provides growth and colonization advantages for K. pneumoniae *in the inflamed gut*

The genome of *K. pneumoniae* encodes two nitrate reductases, NarGHI and NarZYV [28]. To determine whether nitrate respiration confers a fitness advantage upon *K. pneumoniae*, we constructed the single mutant strains Δ*narG*, Δ*narZ*, and double mutant Δ*narG*Δ*narZ*. *In vitro* analysis of these mutants cultured anaerobically in the presence of nitrate showed that Δ*narG* and Δ*narG*Δ*narZ* exhibited severe growth defects and lacked nitrate reductase activity. In contrast, no significant difference in anaerobic growth or nitrate reductase activity was observed between Δ*narZ* and WT (Figure 4(a-b)). Additionally, the competitive anaerobic growths of Δ*narG* and Δ*narG*Δ*narZ* were strongly outcompeted by the WT strain in the presence of nitrate ($p < 0.01$), whereas the competitive anaerobic growth of Δ*narZ* was not significantly affected by the addition of nitrate (Figure 4(c)). The competitive

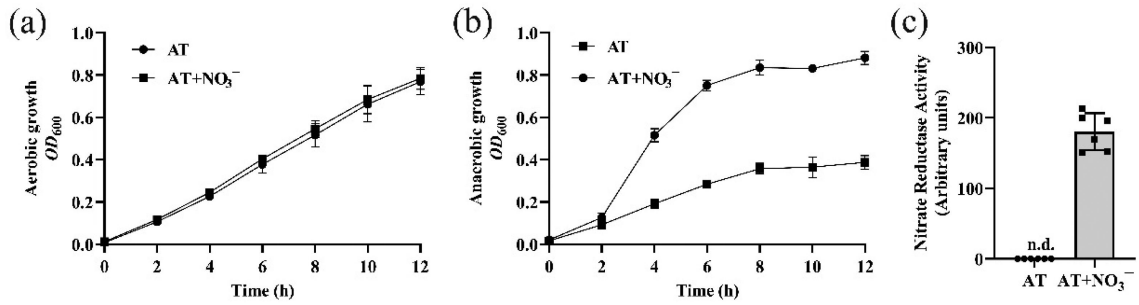

Figure 3. Impact of intestinal nitrate on aerobic and anaerobic growth of *K. pneumoniae in vitro*. (a) The WT strain was grown aerobically in at medium supplemented with or without 20 mm KNO_3 for 12 h, and the growth was monitored by the change in OD_{600} every 2 h. (b) Anaerobic growth curve of the WT strain in at medium supplemented with or without 20 mm KNO_3. (c) Nitrate reductase activity of the WT strain was measured after 3 h of anaerobic culture. Data are represented as means ± standard deviations (error bars) of three independent experiments. n.D., not detectable.

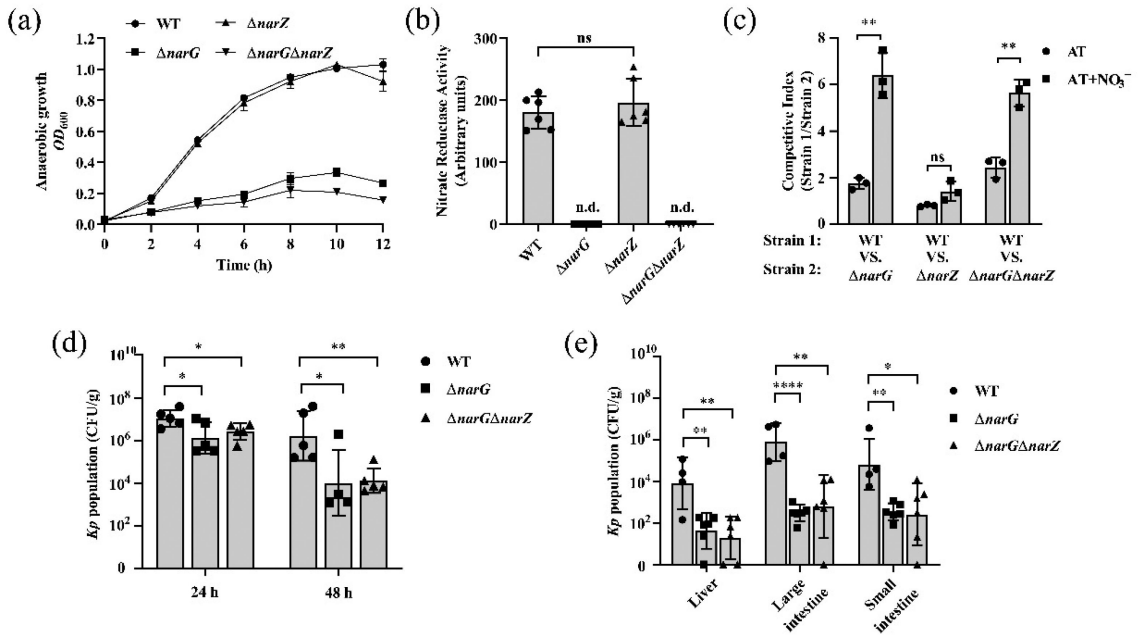

Figure 4. Nitrate respiration enhances the fitness of *K.* pneumoniae during gut inflammation. (a) Strains WT, Δ*narG*, Δ*narZ, and* Δ*narG*Δ*narZ* were grown anaerobically in AT medium supplemented with 20 mm KNO_3 for 12 h, and the anaerobic growth was monitored by the change in OD_{600}. (b) Nitrate reductase activity of the WT and mutant strains (Δ*narG*, Δ*narZ*, and Δ*narG*Δ*narZ*) after 3 h of anaerobic culture. (c) The competitive index of K. pneumoniae WT (green fluorescence) and the deletion mutants Δ*narG*, Δ*narZ*, or Δ*narG*Δ*narZ* (red fluorescence) after 24 h anaerobic growth in AT medium with or without 20 mm KNO_3. The index was determined as the CFU ratio of recovered WT to deletion mutants. (d) Fecal bacterial counts at 24 and 48 h post-inoculation of 10^9 CFU of WT, Δ*narG*, or Δ*narG*Δ*narZ* strains into DSS-treated SPF C57BL/6 mice. (e) Bacterial 27 loads in the liver, large intestine, and small intestine tissues 72 h after inoculation. Data are represented as means + standard deviations (Error Bars) of three independent experiments. n.d., not detectable; *,$P < 0.05$; **,$P < 0.01$; ****,$P < 0.0001$; ns, not statistically significant. (unpaired two-tailed Student's *t*-test).

indexes of WT and Δ*narG*, Δ*narZ*, and Δ*narG*Δ*narZ* in the absence of nitrate were approximately 1.73, 0.79, and 2.43, respectively, suggesting that the mutants Δ*narG* and Δ*narG*Δ*narZ* exhibit slight intrinsic growth defects (Figure 4(c)). These data confirm that the nitrate reductase NarG is the major contributor to nitrate reduction in *K. pneumoniae*.

Next, we assessed whether nitrate respiration provides a colonization advantage for *K. pneumoniae* in the inflamed gut using IBD mouse models. Mice were inoculated with 1×10^9 CFU of WT, Δ*narG*, or Δ*narG*Δ*narZ* strains. The WT strain was found in significantly higher numbers in the faeces of DSS-treated mice compared to the mutant Δ*narG* (24 h:

8-fold, $p = 0.043$; 48 h: 160-fold, $p = 0.0428$) and the double mutant Δ*narG*Δ*narZ* (24 h: 4-fold, $p = 0.0367$; 48 h: 120-fold, $p = 0.0068$) (Figure 4(d)). In addition, the bacterial loads of WT in the liver, large intestine, and small intestine 72 h after inoculation were approximately 190, 2600, and 190 times higher than those of the mutant Δ*narG* with highly significant differences. Similar results were obtained for the double mutant Δ*narG*Δ*narZ* (Figure 4(e)). These results confirm that nitrate respiration, particularly through the *narG* gene, provides both growth and colonization advantages for *K. pneumoniae* in the inflamed gut.

Molybdate transport protein ModA increases the intestinal colonization and extraintestinal dissemination of K. pneumoniae *in the inflamed gut through regulating nitrate reductase activity*

Nitrate reductases are molybdoenzymes containing a molybdenum (Mo) atom complexed with an organic pyranopterin cofactor at their active site [9]. To investigate the role of Mo in nitrate-dependent anaerobic respiration and the pathogenicity of *K. pneumoniae*, we created a mutant lacking the gene encoding the molybdate-binding protein ModA. Anaerobic growth curves of the Δ*modA* mutant were compared to the WT strain in AT medium supplemented with or without 20 mm KNO_3. The Δ*modA* did not exhibit significant anaerobic growth and nitrate reductase activity when supplemented with 20 mm KNO_3, while restored in C-*modA* (Figure 5(a-b)). The study showed that lower nitrate reductase activity could hinder *K. pneumoniae*'s anaerobic growth due to a lack of intracellular Mo accumulation. To confirm this, we assessed the anaerobic growth and nitrate reductase activity of WT and Δ*modA* strains in AT broth containing 20 mm KNO_3, with or without 100 μM Na_2MoO_4. The results showed that sufficient extracellular Mo restored the intracellular Mo accumulation and facilitated the nitrate-dependent anaerobic growth of Δ*modA* (Figure 5(c-d)). The results indicate that the molybdate transport protein ModA associates with the anaerobic growth of *K. pneumoniae* through influencing molybdate acquisition from the environment.

Next, the growth, colonization and pathogenicity of WT, Δ*modA* and C-*modA* strains were assessed in DSS-treated mice through intragastric inoculation with 1×10^9 CFU of each strain. At 24 and 48 h post-inoculation, the faecal bacterial counts of the WT strain were significantly higher than those of the Δ*modA* mutant (24 h: 35-fold, $P = 0.0261$; 48 h: 420-fold, $P = 0.0002$). No significant differences were observed between WT and C-*modA* (24 h: 1-fold, $p = 0.7058$; 48 h: 0.8-fold, $P = 0.8569$) (Figure 5(e)). At 72 h, the cells of Δ*modA* were nearly undetectable (20 CFU/mL) in the liver and most large intestine and small intestine contents of DSS-treated mice (Figure 5(f)). Taken together, these findings suggest that the molybdate transport protein ModA regulates nitrate reductase activity to increase the intestinal colonization and extraintestinal dissemination of *K. pneumoniae* in the inflamed gut.

Tungstate treatment abrogates the fitness advantage of K. pneumoniae *in the inflamed gut by inhibiting nitrate respiration*

Since ModA is required for anaerobic nitrate reduction for *in vitro* growth, *in vivo* robust intestinal colonization and extraintestinal dissemination of *K. pneumoniae*, we speculate that ModA may be a promising drug target. Tungsten competes with Mo for ModA binding and can replace Mo in the MoCo, thus inhibiting MoCo-dependent processes during gut inflammation [21]. To investigate this, we analysed the competitive anaerobic growth and nitrate reductase activity of WT, Δ*modA* and C-*modA* strains in AT broth supplemented with tungstate. The addition of tungstate reduced the competitive index of WT and Δ*modA* after 24 h of anaerobic growth, from 4.8 to 0.89 (Figure 6(a)). Furthermore, tungstate significantly decreased the nitrate reductase activities of WT and C-*modA* strains (Figure 6(b)), demonstrating that tungstate inhibits the growth advantage of *K. pneumoniae* conferred by nitrate respiration *in vitro*.

The effect of tungstate were further evaluated in the DSS-induced IBD mouse model. Tungstate-treated mice (DSS+WO_4^{2-}) exhibited significantly reduced WT bacterial counts in faecal contents compared to the control group (DSS) (24 h: 3-fold, $p = 0.0418$; 48 h: 30-fold, $p = 0.0036$) (Figure 6(c)). Additionally, tungstate treatment markedly reduced bacterial loads in the liver, large intestine, and small intestine of mice at 72 h post-inoculation (Figure 6(d)). These findings suggest that tungstate administration in the DSS-induced-colitis model abrogates the fitness advantage of *K. pneumoniae* during gut inflammation by inhibiting nitrate respiration, thereby highlighting ModA as a promising therapeutic target.

Discussion

IBD is a group of chronic, patchy, and remittent gastrointestinal inflammatory diseases with an elusive aetiology caused by a combination of genetic, immunological, microbial, and environmental factors [29,30]. Over the past decades, Adherent-invasive *E. coli*, *Salmonella* species, *Clostridium difficile* and

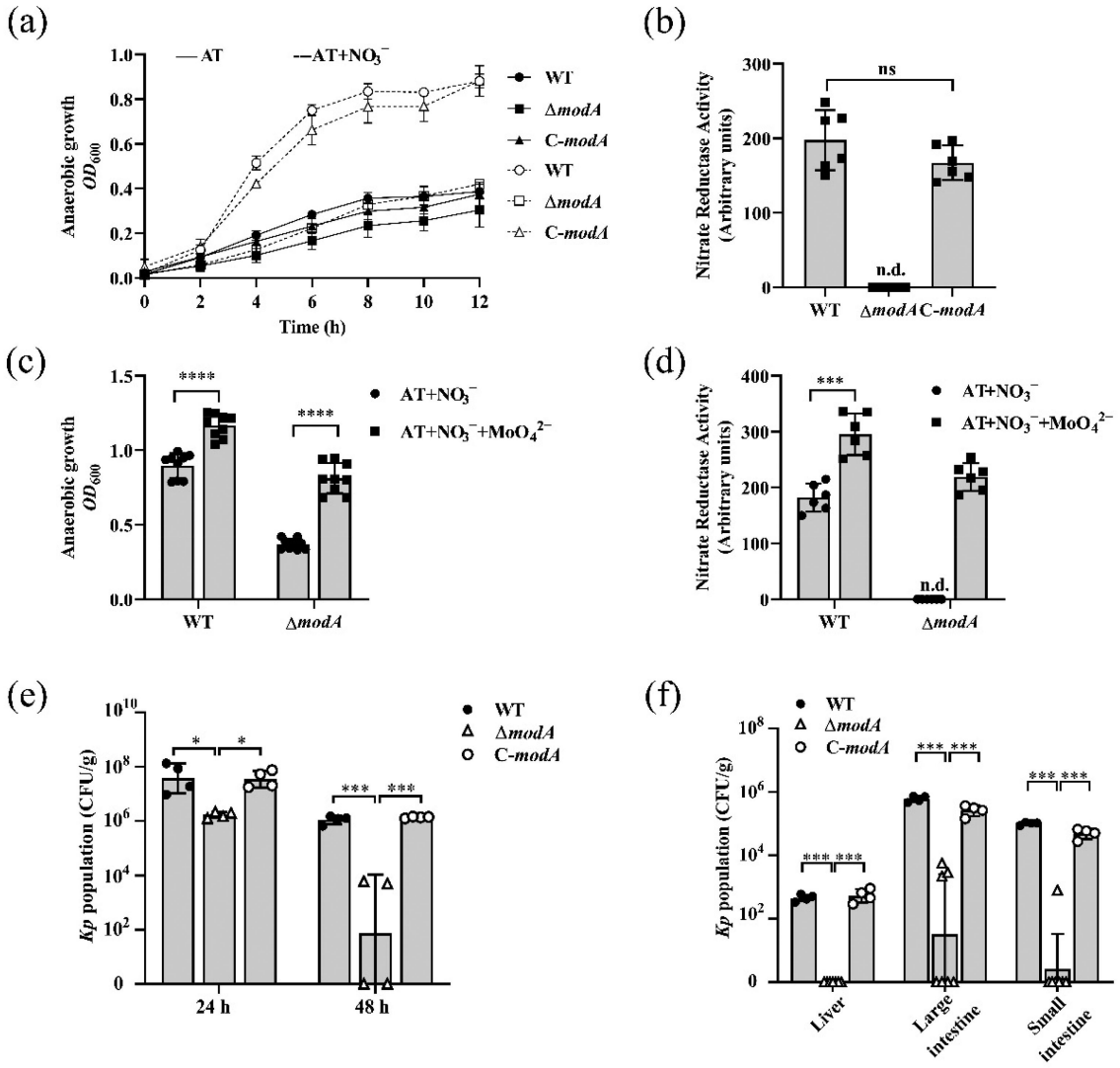

Figure 5. ModA regulates the nitrate reductase activity to enhance the fitness of *K. pneumoniae* during gut inflammation. (a) Strains WT, Δ*modA* and C-*modA* were grown anaerobically in at medium supplemented with or without 20 mm KNO_3 for 12 h, and the anaerobic growth was monitored by the change in OD_{600}. (b) Nitrate reductase activity of WT, Δ*modA*, and C-*modA* strains after 3 h of anaerobic culture in at broth containing 20 mm KNO_3. (c) Anaerobic growth of WT and Δ*modA* strains in at broth containing 20 mm KNO_3 with or without 100 μm Na_2MoO_4 for 24 h. (d) Nitrate reductase activity of WT and Δ*modA* strains after 3 h of anaerobic growth in at broth containing 20 mm KNO_3 with or without 100 μm Na_2MoO_4. (e) Fecal bacterial counts of dss-treated SPF C57BL/6 mice at 24 and 48 h post-inoculation of 10^9 CFU of WT, Δ*modA* or C-*modA* strains. (f) Bacterial loads in the liver, large intestine, and small intestine tissues of dss-treated mice 72 h after inoculation with WT, Δ*modA* or C-*modA* strains. Data are represented as means ± standard deviations (error bars). n.d., not detectable; *, $p < 0.05$; ***, $p < 0.001$; ****, $p < 0.0001$; ns, not statistically significant (b-d: unpaired two-tailed Student's *t*-test; e-f: one way ANOVA).

K. pneumoniae have been implicated in the pathogenesis of IBD [31–33]. At the same time, patients with IBD exhibit a significantly higher incidence and severity of infections caused by *E. coli* and *S. typhimurium* compared to healthy individuals [6].

K. pneumoniae is a gram-negative bacterium found in diverse ecological niches and the mouth, skin, and intestine of mammals. The prevalence of gastrointestinal carriage of *K. pneumoniae* and the incidence of pyogenic liver abscess infections have increased in patients with IBD [34,35]. Several studies have revealed that *K. pneumoniae* infection can induce intestinal inflammation in a gut microbiota-dependent manner and exacerbate colitis in murine models of IBD [36–39]. Our study confirmed that the *K. pneumoniae* number was raised in the caecal content, liver, large intestine, and small intestine of DSS-induced-colitis mice inoculated with bacteria than in mock-treated mice. The results prove that IBD is a risk factor for *K. pneumoniae* infection and changes in the intestinal microenvironment

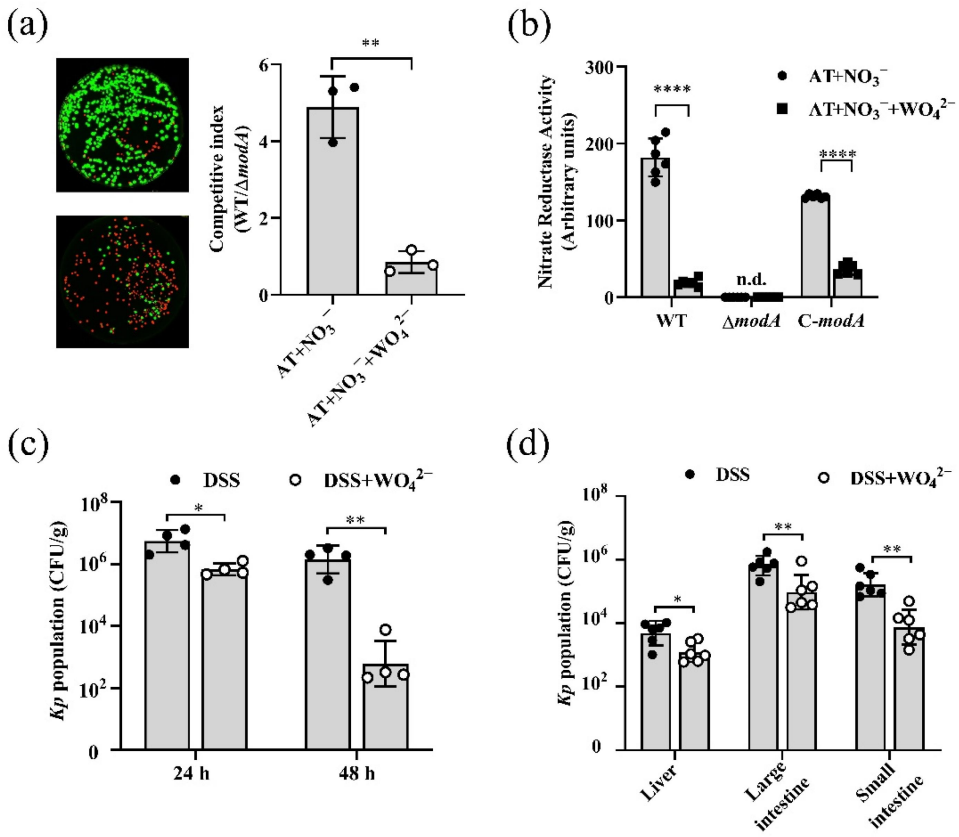

Figure 6. Effect of tungstate treatment on nitrate respiration and fitness advantage of *K. pneumoniae* during gut inflammation.(a) The competitive index of *K. pneumoniae* WT (green fluorescence) and Δ*modA* (red fluorescence) strains after 24h of anaerobic growth in at broth containing 20mM KNO_3 with or without 10mM Na_2WO_4. The competitive index was calculated as the ratio of CFU recovered for WT to that of Δ*modA*.(b) Nitrate reductase activity of WT, Δ*modA*, and C-*modA* strains after 3h of anaerobic growth in at broth supplemented with 20mM KNO_3, with or without 10mM Na_2WO_4.(c) Groups of SPF C57BL/6 mice were administered 3% DSS (DSS) or 3% DSS plus 0.2% Na_2WO_4 (DSS+WO_4^{2-}) and then were inoculated intragastrically with 10^9 CFU of *K. pneumoniae* WT strain on day 5. Fecal bacterial counts were determined at 24h and 48h post-inoculation.(d) Bacterial loads in the liver, large intestine, and small intestine tissues of dss-treated mice 72h post- inoculation with WT strain, in the presence or absence of Na_2WO_4. Data are represented as means±standard deviations (error bars). n.d., not detectable; *, $p<0.05$; **, $p<0.01$; ****, $p<0.0001$ (a: paired two-tailed Student's *t*-test; b-d: unpaired two-tailed Student's *t*-test)

of IBD patients promote the growth, intestinal colonization and extraintestinal dissemination of *K. pneumoniae*.

Nitrate is one of the by-products of gut inflammatory response, and its levels were increased in the caecal mucus layer of DSS-treated mice. The effect of increased nitrate levels in the gut varies among bacterial species depending on their ability to utilize it. Previous studies have shown that nitrate in the inflamed gut boosts the growth of *E. coli* and *S. Typhimurium*, but provides no apparent benefit for *Vibrio cholerae* [6,40,41]. For *K. pneumoniae*, the addition of nitrate to the medium significantly increased the anaerobic growth and nitrate reductase activity *in vitro*, suggesting that *K. pneumoniae* could use nitrate and might confer a growth advantage in the inflamed gut. Unlike *E. coli*, *K. pneumoniae* has only NarGHI and NarZYV nitrate reductases, lacking the periplasmic nitrate reductase NapABC. The anaerobic growth curve and the competitive anaerobic growth of the single mutant strains Δ*narG*, Δ*narZ*, and double mutant Δ*narG*Δ*narZ* with wild-type strain in AT broth in the presence of nitrate found the nitrate reductase NarG is the major contributor to nitrate reduction in *K. pneumoniae*. Strains with an inactivated *narG* gene exhibited a complete loss of nitrate reductase activity and had significantly more colonization defects in DSS-treated mice compared to the wild-type strain. In conclusion, nitrate respiration contributes to the intestinal lifestyle, the ability of intestinal colonization and extraintestinal dissemination of *K. pneumoniae*.

K. pneumoniae is one of the bacteria that is easily resistant to the antibiotics used today [42–44]. How to impair growth and colonization in the intestinal tract is a problem in mitigating severe infections of *K. pneumoniae* in IBD patients. The reduction of nitrate reductase activity can decrease *K. pneumoniae* in the gut. Metal-based antibacterial agents are emerging as novel antimicrobial strategies. Nitrate reductases are molybdoenzymes that contain a single Mo atom at their active site [45–47]. For efficient uptake of molybdate from the gastrointestinal microenvironment, bacteria rely on the high-affinity Mo uptake system ModABC. In *S. typhi* and *P. aeruginosa*, ModABC has been identified as essential for host interactions [15,48,49]. Our study demonstrates that the *modA* gene, which encodes the molybdate-binding protein of ModABC, is crucial for *K. pneumoniae*'s *in vitro* growth under anaerobic conditions through nitrate reduction. ModA increases the intestinal colonization and extraintestinal dissemination of *K. pneumoniae* in the inflamed gut by regulating the nitrate reductase activity.

Tungsten is an element that competes with Mo to bind ModA and could inhibit MoCo-dependent processes in the inflamed gut to improve colitis [21]. Tungstate supplementation has been shown to inhibit the anaerobic growth of *E. coli* and *P. aeruginosa* [15,21]. Similarly, the addition of tungstate to nitrate-containing AT medium decreased the growth of *K. pneumoniae*. Administration of tungstate in the DSS-induced-colitis model abrogated the fitness advantage of *K. pneumoniae*, suggesting that tungstate may serve as an alternative selection to decrease the *K. pneumoniae* growth, colonization and infection in the gut. However, sodium tungstate primarily localizes to bone and spleen following oral administration, which induces DNA damage in the bone marrow [50,51]. To overcome these limitations, advanced tungsten-based delivery systems have been developed. Colonic mucus-accumulating tungsten oxide nanoparticles improve therapeutic efficacy against colitis by increasing the adherence of tungsten with Enterobacteriaceae, compared to sodium tungstate [52]. A calcium tungstate microgel encapsulated probiotics effectively treats colitis by releasing tungsten selectively to inhibit Enterobacteriaceae while promoting probiotics colonization [53]. Additionally, recent research reveals that tungstate exerts potentiating effects on gentamicin and ciprofloxacin against *E. coli* [54]. The effect of tungstate-based materials or tungstate-antibiotics combinations on the treatment of *K. pneumoniae* infections needs to be further studied.

Collectively, our findings demonstrate that nitrate confers a significant growth advantage to *K. pneumoniae* in the intestine of DSS-treated mice, and the molybdate transport protein ModA plays a critical role in regulating nitrate reductase activity to increase the growth, intestinal colonization and extraintestinal dissemination of *K. pneumoniae*. Tungstate emerges as a promising antibacterial agent to tackle *K. pneumoniae* infections in IBD patients. This study will contribute to elucidating the impact of nitrate on the growth and pathogenicity of *K. pneumoniae* in the inflamed gut, providing a theoretical basis for the treatment of *K. pneumoniae* infection in IBD patients in the future.

Acknowledgements

The authors would like to express their gratitude to EditSprings (https://www.editsprings.cn) for the expert linguistic services provided.

Disclosure statement

No potential conflict of interest was reported by the author(s).

Funding

This work was supported by Hubei Province's Outstanding Medical Academic Leader Program; the Innovative Research Program for Graduates of Hubei University of Medicine [YC2023025]; the Cultivating Project for Young Scholar at Hubei University of Medicine [2021QDJZR021] and the Advantages Discipline Group (Public health) Project in Higher Education of Hubei Province [2021–2025].

Author contributions

Conception and design of study: Jichen Xie, Hui Wang.

Acquisition of data: Jichen Xie, Hui Wang, Renhui Ma.

Data analysis and/or interpretation: Renhui Ma, Qiuhang Quan, Zhiqiang Zhang.

Drafting of manuscript and/or critical revision: Jichen Xie, Jinming Fan, Moran Li, Bei Li.

Approval of final version of manuscript: Moran Li, Bei Li.

All authors agree to be responsible for all aspects of their work.

Data availability statement

All data in this article will be obtained through http://doi.org/10.57760/sciencedb.12381.

ORCID

Moran Li http://orcid.org/0000-0001-9549-2797

References

[1] Gorrie CL, Mirceta M, Wick RR, et al. Gastrointestinal carriage is a major reservoir of *Klebsiella pneumoniae* infection in intensive care patients. Clin Infect Dis. 2017;65(2):208–215. doi: 10.1093/cid/cix270

[2] Yang J, Li Y, Tang N, et al. The human gut serves as a reservoir of hypervirulent *Klebsiella pneumoniae*. Gut Microbes. 2022;14(1):24739. doi: 10.1080/10976.2022.24739

[3] Xu Q, Yang X, Chan EWC, et al. The hypermucoviscosity of hypervirulent *K. pneumoniae* confers the ability to evade neutrophil-mediated phagocytosis. Virulence. 2021;12(1):2050–2059. doi: 10.1080/25594.2021.10101

[4] Liu R, Xu H, Zhao J, et al. Emergence of mcr-8.2-harboring hypervirulent ST412 *Klebsiella pneumoniae* strain from pediatric sepsis: a comparative genomic survey. Virulence. 2023;14(1):233–245. doi: 10.1080/25594.2022.28980

[5] Bueno E, Mesa S, Bedmar EJ, et al. Bacterial adaptation of respiration from oxic to microoxic and anoxic conditions: redox control. Antioxid Redox Signal. 2012;16(8):819–852. doi: 10.1089/ars.2011.4051

[6] Winter SE, Winter MG, Xavier MN, et al. Host-derived nitrate boosts growth of *E. coli* in the inflamed gut. Science. 2013;339(6120):708–711. doi: 10.1126/science.12467

[7] Spees AM, Wangdi T, Lopez CA, et al. Streptomycin-induced inflammation enhances *Escherichia coli* gut colonization through nitrate respiration. MBio. 2013;4(4). doi: 10.1128/mBio.00430-13

[8] Lopez CA, Rivera-Chavez F, Byndloss MX, et al. The periplasmic nitrate reductase NapABC supports luminal growth of *Salmonella enterica* serovar typhimurium during colitis. Infect Immun. 2015;83(9):3470–3478. doi: 10.1128/IAI.00351-15

[9] Liu H, Huang Y, Huang M, et al. From nitrate to NO: potential effects of nitrate-reducing bacteria on systemic health and disease. Eur J Med Res. 2023;28(1):425. doi: 10.1186/s0001-023-01413-y

[10] Durand S, Guillier M. Transcriptional and post-transcriptional control of the nitrate respiration in bacteria. Front Mol Biosci. 2021;8:67758. doi: 10.3389/fmolb.2021.67758

[11] Chen X, Liu C, Zhu B, et al. The contribution of nitrate dissimilation to nitrate consumption in *narG*- and *napA*-containing nitrate reducers with various oxygen and nitrate supplies. Microbiol Spectr. 2022;10(6):e9522. doi: 10.1128/spectrum.00695-22

[12] Rech S, Deppenmeier U, Gunsalus RP. Regulation of the molybdate transport operon, *modABCD*, of *Escherichia coli* in response to molybdate availability. J Bacteriol. 1995;177(4):1023–1029. doi: 10.1128/jb.177.4.1023-1029.1995

[13] Huang Y, Chen J, Jiang Q, et al. The molybdate-binding protein ModA is required for *proteus mirabilis*-induced UTI. Front Microbiol. 2023;14:16273. doi: 10.3389/fmicb.2023.16273

[14] Xia Z, Lei L, Zhang HY, et al. Corrigendum: characterization of the ModABC molybdate transport system of *Pseudomonas putida* in nicotine degradation. Front Microbiol. 2018;9:3213. doi: 10.3389/fmicb.2018.03213

[15] Pederick VG, Eijkelkamp BA, Ween MP, et al. Acquisition and role of molybdate in *Pseudomonas aeruginosa*. Appl Environ Microbiol. 2014;80(21):6843–6852. doi: 10.1128/AEM.02465-14

[16] Zhao Q, Su X, Wang Y, et al. Structural analysis of molybdate binding protein ModA from *Klebsiella pneumoniae*. Biochem Biophys Res Commun. 2023;681:41–46. doi: 10.1016/j.bbrc.2023.09.055

[17] Raffelsberger N, Hetland MAK, Svendsen K, et al. Gastrointestinal carriage of *Klebsiella pneumoniae* in a general adult population: a cross-sectional study of risk factors and bacterial genomic diversity. Gut Microbes. 2021;13(1):19599. doi: 10.1080/10976.2021.19599

[18] Lin JN, Lin CL, Lin MC, et al. Pyogenic liver abscess in patients with inflammatory bowel disease: a nationwide cohort study. Liver Int. 2016;36(1):136–144. doi: 10.1111/liv.12875

[19] Kaur CP, Vadivelu J, Chandramathi S. Impact of *Klebsiella pneumoniae* in lower gastrointestinal tract diseases. J Dig Dis. 2018;19(5):262–271. doi: 10.1111/1751-2980.12595

[20] Aguilar-Barajas E, Diaz-Perez C, Ramirez-Diaz MI, et al. Bacterial transport of sulfate, molybdate, and related oxyanions. Biometals. 2011;24(4):687–707. doi: 10.1007/s0534-011-9421-x

[21] Zhu W, Winter MG, Byndloss MX, et al. Precision editing of the gut microbiota ameliorates colitis. Nature. 2018;553(7687):208–211. doi: 10.1038/nature5172

[22] Wu KM, Li LH, Yan JJ, et al. Genome sequencing and comparative analysis of *Klebsiella pneumoniae* NTUH-K2044, a strain causing liver abscess and meningitis. J Bacteriol. 2009;191(14):4492–4501. doi: 10.1128/JB.00315-09

[23] Izquierdo L, Coderch N, Pique N, et al. The *Klebsiella pneumoniae wabG* gene: role in biosynthesis of the core lipopolysaccharide and virulence. J Bacteriol. 2003;185(24):7213–7221. doi: 10.1128/JB.185.24.7213-7221.2003

[24] Pan YJ, Fang HC, Yang HC, et al. Capsular polysaccharide synthesis regions in *Klebsiella pneumoniae* serotype K57 and a new capsular serotype. J Clin Microbiol. 2008;46(7):2231–2240. doi: 10.1128/JCM.01716-07

[25] Wang H, Li F, Xu L, et al. Contributions of *Escherichia coli* and its motility to the formation of dual-species biofilms with *Vibrio cholerae*. Appl Environ Microbiol. 2021;87(18):e3821. doi: 10.1128/AEM.00938-21

[26] Ou Q, Fan J, Duan D, et al. Involvement of cAMP receptor protein in biofilm formation, fimbria production, capsular polysaccharide biosynthesis and lethality in mouse of *Klebsiella pneumoniae* serotype K1 causing pyogenic liver abscess. J Med Microbiol. 2017;66(1):1–7. doi: 10.1099/jmm.0.00391

[27] Hughes ER, Winter MG, Duerkop BA, et al. Microbial respiration and formate oxidation as metabolic signatures of inflammation-associated dysbiosis. Cell Host & Microbe. 2017;21(2):208–219. doi: 10.1016/j.chom.2017.01.005

[28] Pal RR, Khardenavis AA, Purohit HJ. Identification and monitoring of nitrification and denitrification genes in *Klebsiella pneumoniae* EGD-HP19-C for its ability to perform heterotrophic nitrification and aerobic denitrification. Funct Integr Genomics. 2015;15(1):63–76. doi: 10.1007/s0142-014-0406-z

[29] Kamada N, Seo SU, Chen GY, et al. Role of the gut microbiota in immunity and inflammatory disease. Nat Rev Immunol. 2013;13(5):321–335. doi: 10.1038/nri3430
[30] Baumgart DC, Carding SR. Inflammatory bowel disease: cause and immunobiology. The Lancet. 2007;369 (9573):1627–1640. doi: 10.1016/S0140-6736(07)60750-8
[31] Palmela C, Chevarin C, Xu Z, et al. Adherent-invasive *Escherichia coli* in inflammatory bowel disease. Gut. 2018;67(3):574–587. doi: 10.1136/gutjnl-2017-34903
[32] Axelrad JE, Cadwell KH, Colombel JF, et al. Systematic review: gastrointestinal infection and incident inflammatory bowel disease. Aliment Pharmacol Ther. 2020;51(12):1222–1232. doi: 10.1111/apt.15770
[33] Federici S, Kredo-Russo S, Valdes-Mas R, et al. Targeted suppression of human ibd-associated gut microbiota commensals by phage consortia for treatment of intestinal inflammation. Cell. 2022;185(16):-2879–2898 e2824.doi: 2879–2898.e24. doi: 10.1016/j.cell.2022.07.003
[34] Ko WC, Paterson DL, Sagnimeni AJ, et al. Community-acquired *Klebsiella pneumoniae* bacteremia: global differences in clinical patterns. Emerg Infect Dis. 2002;8 (2):160–166. doi: 10.3201/eid0802.00025
[35] Shimasaki T, Seekatz A, Bassis C, et al. Increased relative abundance of *Klebsiella pneumoniae* carbapenemase-producing *Klebsiella pneumoniae* within the gut microbiota is associated with risk of bloodstream infection in long-term acute care hospital patients. Clin Infect Dis. 2019;68(12):2053–2059. doi: 10.1093/cid/ciy796
[36] Lee IA, Kim DH. *Klebsiella pneumoniae* increases the risk of inflammation and colitis in a murine model of intestinal bowel disease. Scand J Gastroenterol. 2011;46 (6):684–693. doi: 10.3109/05521.2011.50678
[37] N A-F, M B-J, Cheng C, et al. Exploring the role of *Klebsiella variicola* and *Klebsiella pneumoniae* in pediatric ulcerative colitis pathogenesis. J Can Assoc Of Gastroenterol. 2024;7(Supplement_1):142–143. doi: gwad061.181
[38] Atarashi K, Suda W, Luo C, et al. Ectopic colonization of oral bacteria in the intestine drives T(H)1 cell induction and inflammation. Science. 2017;358 (6361):359–365. doi: 10.1126/science.aan4526
[39] Zhang Q, Su X, Zhang C, et al. *Klebsiella pneumoniae* induces inflammatory bowel disease through caspase-11-mediated IL18 in the gut epithelial cells. Cell Mol Gastroenterol Hepatol. 2023;15(3):613–632. doi: 10.1016/j.jcmgh.2022.11.005
[40] Winter SE, Thiennimitr P, Winter MG, et al. Gut inflammation provides a respiratory electron acceptor for *salmonella*. Nature. 2010;467(7314):426–429. doi: 10.1038/nature9415
[41] Bueno E, Sit B, Waldor MK, et al. Anaerobic nitrate reduction divergently governs population expansion of the enteropathogen *vibrio cholerae*. Nat Microbiol. 2018;3(12):1346–1353. doi: 10.1038/s1564-018-0253-0
[42] Zhang Q, Zhou H, Jiang P, et al. Metal-based nanomaterials as antimicrobial agents: a novel driveway to accelerate the aggravation of antibiotic resistance. J Hazard Mater. 2023;455(11658):11658. doi: 10.1016/j.jhazmat.2023.11658
[43] Breijyeh Z, Jubeh B, Karaman R. Resistance of gram-negative bacteria to current antibacterial agents and approaches to resolve it. Molecules. 2020;25 (6):1340. doi: 10.3390/molecules61340
[44] Li G, Jia L, Wan L, et al. Acquisition of a novel conjugative multidrug-resistant hypervirulent plasmid leads to hypervirulence in clinical carbapenem-resistant *Klebsiella pneumoniae* strains. mLife. 2023;2(3):317–327. doi: 10.1002/mlf2.12086
[45] Zupok A, Iobbi-Nivol C, Mejean V, et al. The regulation of Moco biosynthesis and molybdoenzyme gene expression by molybdenum and iron in bacteria. Metallomics. 2019;11(10):1602–1624. doi: 10.1039/c9mt0186g
[46] Demtroder L, Narberhaus F, Masepohl B. Coordinated regulation of nitrogen fixation and molybdate transport by molybdenum. Mol Microbiol. 2019;111 (1):17–30. doi: 10.1111/mmi.14152
[47] Leimkuhler S. The biosynthesis of the molybdenum cofactors in *Escherichia coli*. Environ Microbiol. 2020;22(6):2007–2026. doi: 10.1111/1462-2920.15003
[48] Contreras I, Toro CS, Troncoso G, et al. *Salmonella typhi* mutants defective in anaerobic respiration are impaired in their ability to replicate within epithelial cells. Microbiol (Read). 1997;143(Pt 8):2665–2672. doi: 10.1099/01287-143-8-2665
[49] Perinet S, Jeukens J, Kukavica-Ibrulj I, et al. Molybdate transporter ModABC is important for *Pseudomonas aeruginosa* chronic lung infection. BMC Res Notes. 2016;9:23. doi: 10.1186/s3104-016-1840-x
[50] Guandalini GS, Zhang L, Fornero E, et al. Tissue distribution of tungsten in mice following oral exposure to sodium tungstate. Chem Res Toxicol. 2011;24 (4):488–493. doi: 10.1021/tx0011k
[51] Kelly AD, Lemaire M, Young YK, et al. In vivo tungsten exposure alters B-cell development and increases DNA damage in murine bone marrow. Toxicol Sci. 2013;131(2):434–446. doi: 10.1093/toxsci/kfs324
[52] Qin Y, Zhan R, Qin H, et al. Colonic mucus-accumulating tungsten oxide nanoparticles improve the colitis therapy by targeting enterobacteriaceae. Nano Today. 2021;39(1):11234. doi: 10.1016/j.nantod.2021.11234
[53] Yang J, Peng M, Tan S, et al. Calcium tungstate microgel enhances the delivery and colonization of probiotics during colitis via intestinal ecological niche occupancy. ACS Cent Sci. 2023;9(7):1327–1341. doi: 10.1021/acscentsci.3c0227
[54] Silva JC, Moura TF, Pereira RL, et al. FTIR analysis and antimicrobial activity of sodium tungstate and calcium tungstate. Vib Spectrosc. 2021;132(1):13691. doi: 10.1016/j.vibspec.2024.103691